Journal of Materials Physics and Chemistry, 2024, Vol. 12, No. 2, 37-41
Available online at http://pubs.sciepub.com/jmpc/12/2/3
Published by Science and Education Publishing
DOI:10.12691/jmpc-12-2-3

Structural Characterization of P-type SnO_2: Ga and Sb-co-doped SnO2:Ga Thin Films Prepared by Sol-Gel Dip-Coating Method for Potential Optoelectronic Applications

Sally Kemuma Gichana*, David M. Mulati, Timonah N. Soitah

Department of Physics: Jomo Kenyatta University of Agriculture and Technology (JKUAT).
P.O BOX 62000-00200, NAIROBI-KENYA
*Corresponding author: sallygichana22@gmail.com

Received July 29, 2024; Revised August 30, 2024; Accepted September 05, 2024

Abstract This paper delves into the synthesis and characterization of p-type Transparent Conducting Oxides (TCOs), with a specific focus on Gallium-doped tin oxide (SnO2:Ga)and Antimony co-doped Gallium-tin oxide thin films. The films are deposited on blue microscope glass substrates utilizing the sol-gel dip-coating method. The study tackles the challenges related to the application of p-type TCOs, highlighting advancements in electrical performance compared to their n-type counterparts. Structural characterization through X-ray diffraction indicates both crystalline and amorphous nature of the films. Sharp and narrow diffraction peaks confirm the well-defined doped phases of Ga and Sb at atomic substitutional sites of SnO2. Different phases are identified for pure SnO2and Ga-doped SnO2 films. The preferential orientation shifts with doping concentrations. Sb-co-doped SnO2 films show the highest peak intensities. The average crystallite sizes of the thin films increase with doping concentrations, ranging from 19.83 nm to 32.24 nm for Ga-doped films and 33.91 nm to 40.88 nm for Sb-co-doped films. The structural analyses suggest that SnO2:Ga and Sb-co-doped SnO2:Ga thin films are suitable p-type TCO materials for optoelectronic applications. Overall, this research contributes valuable insights into improving the performance of p-type TCOs and addresses the limitations associated with their characterization.

Keywords: *P-type, Thin Films, Sol-Gel, Structural properties*

Cite This Article: Sally Kemuma Gichana, David M. Mulati, and Timonah N. Soitah, "Structural Characterization of P-type SnO_2:Ga and Sb-co-doped SnO2:Ga Thin Films Prepared by Sol-Gel Dip-Coating Method for Potential Optoelectronic Applications." *Journal of Materials Physics and Chemistry*, vol. 12, no. 2 (2024): 37-41. doi: 10.12691/jmpc-12-2-3.

1. Introduction

Transparent Conductive Oxides (TCOs) constitute a unique class of materials characterized by appreciable electrical conductivity, high optical transparency in the visible range, and significant infrared reflectivity [1]. Their distinctive properties underpin advancements in technology such as touch screen displays, solid-state sensors, organic light emitting diodes (OLEDs), liquid crystal displays, and photovoltaic cells [2,3]. However, unlike their n-type counterparts, the establishment of suitable p-type TCOs remains a challenge [4,5,6]. The complexity arises from the electronic configuration of oxide materials, where the Valence Band Maximum (VBM), the transport path for holes in p-type TCOs, is localized and anisotropic, leading to high hole effective mass and low hole mobility [7,8].

This difficulty impedes the formation of p-n junctions critical for various optoelectronic applications [9]. Despite these challenges, efforts guided by chemical design principles have led to the discovery of several p-type TCOs, including copper-bearing oxides ($CuMO_2$, M=Al, Ga, In), binary copper oxides (CuO and Cu_2O), and zinc spinel oxides [10,11]. Notably, Copper Aluminium oxide ($CuAlO_2$) has shown promise as a highly transparent p-type TCO, although its resistivity remains higher compared to n-type indium tin oxide [10,11] Zinc, when doped or deposited under specific conditions, also exhibits p-type TCO characteristics, albeit with challenges related to rapid decay due to the self-compensation effect [12].

The inadequacy of current p-type TCOs has repercussions, particularly in transparent electronic devices like solar cells, where stability and efficiency are compromised. Substituting p-type TCOs with semi-crystalline metallic organic materials has resulted in reduced device stability and efficiency [13,14,15]. Addressing this gap in suitable p-type TCOs could enable the fabrication of transparent p-n junctions for diverse applications in the transparent electronic industry [13,14,15].

Tin (IV) oxide stands out among TCOs due to its

unique performance and versatility in optoelectronic industry and green energy devices [3,9,16]. SnO_2, an n-type semiconductor with a direct band gap of 3.6 eV to 4.0 eV, finds applications in gas sensors, solar cells, LEDs, transistors, and photo detectors [17,18,19]. Various studies have explored the fabrication of p-type tin-based films, particularly using group (III) elements such as Al and Ga, owing to their unique structures and sizes [20,21]. For instance, the smaller radius of Ga compared to Sn enhances the solubility of Ga ions into the tin site, facilitating p-type conductivity [21,22,23,24,25,26,27].

However, high resistivity due to low intrinsic carrier density and mobility poses a challenge for SnO_2 thin films in achieving p-type conductivity. Co-doping with Sb is proposed to produce thermally and chemically stable materials, as Sb acts as an acceptor at certain doping levels [28,29,30].

Various deposition techniques have been employed for tin-based thin films, including DC and RF magnetron sputtering, spray pyrolysis, chemical vapor deposition sputtering, thermal evaporation, pulsed laser deposition, and the sol-gel method [22,31,32,33,34,35]. Among these, the sol-gel method offers advantages such as cost-effectiveness, environmental friendliness, ease of controlling underlying materials and doping concentrations, low temperature requirements for film densification, and the formation of homogeneous structures [35,36,37].

In this study, transparent p-type conductive thin films of tin doped with Gallium and co-doped with Sb are prepared using the sol-gel dip-coating method, grown on Blue-plus microscope glass slides. Their structural properties are characterized for potential applications in transparent electronics.

2. Experimental

2.1. Materials

Tin (IV) chloride of trace metal basis (99.95 % purity) Sigma Aldrich, Gallium (III) chloride, ultra dry, 99.999 % purity (metal basis) Sigma Aldrich, Ethanol and acetone (solvents) Antimony (III) ethoxide, co-dopant, (99.999 % purity) Sigma Aldrich were used for sol preparations. The Blue plus microscope glass slides were used as the substrates for sol coatings.

2.2. Methods

2.2.1. Preparation of SnO_2:Ga sol

$GaCl_3$-ultra dry, was dissolved in Acetyl acetone at room temperature. Table 1 illustrates the concentration composition values of SnO_2:Ga and Sb-co-doped SnO_2:Ga with the obtained thin films. At various concentration weights; 0.25 g, 0.5 g, 0.75 g and 1.0 g of Ga, the solution was refluxed at 70° C using a reflux set-up for 2 hours to ensure effective homogenization. Hydrated $SnCl_4$ was then dissolved in ethanol in another beaker with the help of a magnetic stirrer at room temperature, cooled down and the solution added drop wise to the Ga dissolved solution. The sol was then aged in the dark room for 7 days [36] as in the flow chart in Figure 1 which illustrates the dissolving, refluxing and aging of the sol.

Table 1. The concentration composition values of SnO_2:Ga and Sb-co-doped SnO_2:Ga

Thin Film name	Concentration weight
Undoped (Sn)	1.2 ml
A (Sn + Ga	1.2 ml + 0.25 g
B (Sn + Ga)	1.2 ml + 0.5 g
C (Sn + Ga)	1.2 ml + 0.75 g
D (Sn + Ga)	1.2 ml + 1.0g
E (Sn + Ga + Sb	1.2 ml + 0.25 g + 0.5 ml
F (Sn + Ga + Sb)	1.2 ml + 0.5 g + 1.0 ml
G (Sn + Ga + Sb)	1.2 ml + 0.75 g + 1.5 ml
H (Sn + Ga + Sb)	1.2 ml + 1.0 g + 2.0 ml

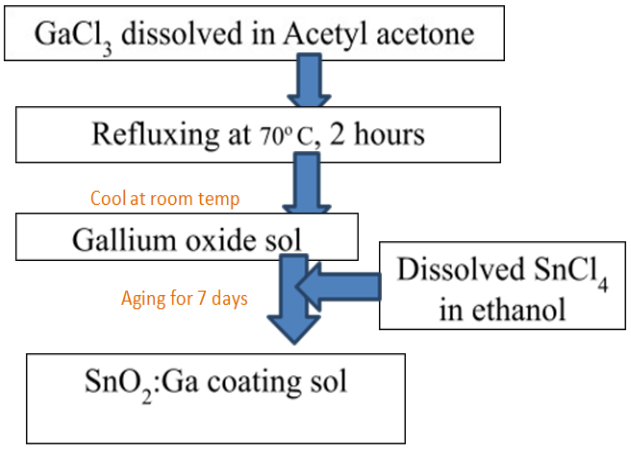

Figure 1. Flow chart of Preparation of SnO_2: Ga sol

2.2.2. Preparation of Sb-co-doped SnO_2: Ga sol

After preparation of the gallium oxide sol, Antimony (III) Ethoxide was added in various concentrations of 0.5 ml, 1.0 ml, 1.5 ml and 2.0 ml (Table 1). The solution was then aged for 7 days to obtain the Sb-co-doped SnO_2:Ga coating sols as shown in flow chart in Figure 2 which illustrates the dissolving, refluxing, co-doping and aging of the sol.

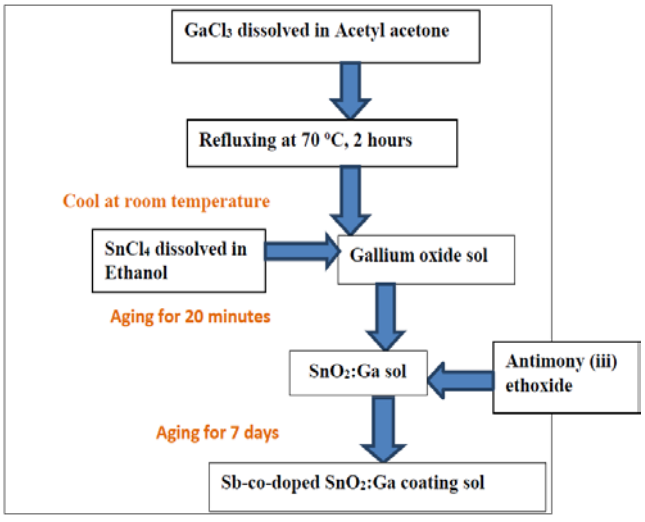

Figure 2. Flow chart of Preparation of Sb-co-doped SnO_2: Ga sol

2.3. Preparation of Glass Substrates

The Blue-Plus microscope glass substrates were used for sol coatings. The substrates were treated ultrasonically in ethanol and acetone and kept in a desiccator, ready for film deposition [38].

2.4. Film Deposition and Subsequent Treatment

Film deposition was carried out in air at room temperature by the dip-coating method (Figure 3) using the cleaned glass substrate. The substrates were left to dry horizontally at 50°C in the oven to remove any organic residuals. The coating-drying procedure was repeated 3-times with an approximated withdrawal speed of 4 cm/min to obtain the desired film thickness [39] The films were then annealed at 150°C (optimal temperature) for 5 minutes and then cooled down at room temperature for crystal formation.

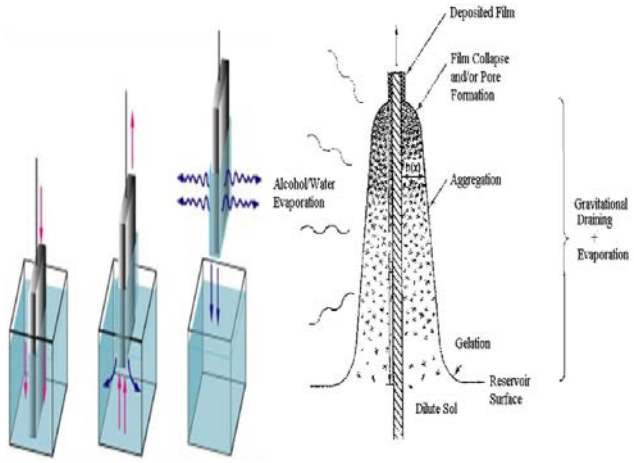

Figure 3. Schematic of the dip-coating and withdrawal of substrate [36]

3. Results and Discussions

3.1. Structural Properties

XRD analysis technique was utilized to determine the crystal structure and crystallinity of the thin films using a Bruker D8 SSS X-Ray diffractometer. X-rays were generated using a Cu source with CuKα radiation (λ=1.5418) at 20kV and 15mA. The grazing incident beam angle was kept at 0.8°. Angular ranges of the patterns collected were between 10 and 70 degrees at a rate of 1 minute per step with a scanning step size of 0.05. XRD spectra were indexed using the originPro85 software. The patterns were analyzed for crystallinity and preferred orientations as shown in Figure 4 and Figure 5.

The presence of fairly sharp and narrow significant diffraction peaks of the prepared thin films indicates the crystalline nature of the films. The doped phases of Ga and Sb were well defined and successfully replaced at atomic substitutional sites of SnO_2.

For pure (undoped) SnO_2 thin film, 4 diffraction peaks were identified as (126), (151), (285) and (407) reflections of the orthorhombic structure. For the Ga doped SnO_2 thin films, the samples related to the monoclinic structure with SnO_2 phases identified due to the mixing of both Ga and SnO_2. The results indicate that the preferential orientation for pure SnO_2 (407) is shifted to (408), (407) and (409) for the Ga-doped SnO_2 and (404), (302), (115) and (408) for the Sb-co-doped SnO_2:Ga. Change of preferred orientation is attributed to the occupancy of additional tin vacancy sites by Ga and Sb sites which were initially unoccupied. The increase in preferred orientation is associated with increase of crystallite growth along that particular plane.

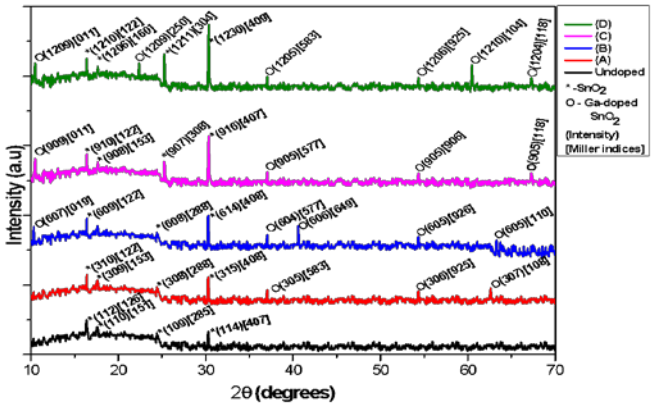

Figure 4. XRD spectra for the undoped (pure) and Ga-doped thin films

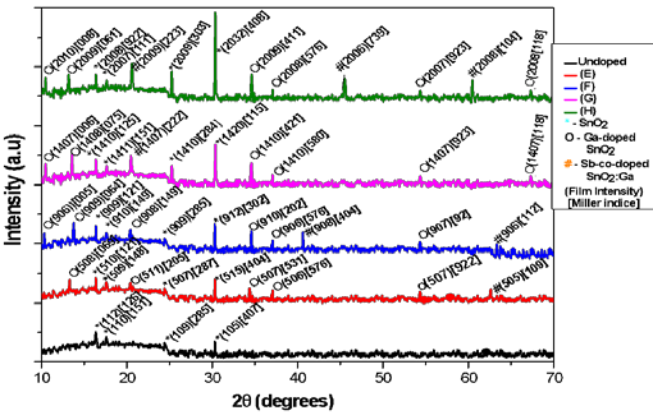

Figure 5. XRD spectra for the undoped (pure) and Sb-co-doped SnO_2:Ga thin films

Increase in peak intensity with film concentration is also observed for all the prepared thin films. All the films indicate one strong peak with the Sb-co-doped thin films registering the highest intensities as compared to the Ga-doped thin films. Thus, the spectra of the films show a well-defined orientation. This can be attributed to an improvement of the films with doping and enhancement in grain sizes. A similar result of increase in peak intensities with doping concentrations and change of preferred orientations is reported by [40] with morphological evaluation of co-precipitated ZnO nanoparticles.

3.2. Structural Parameters of the Prepared Thin Films for Different Ga and Sb Concentrations

The effective grain sizes of the thin films were calculated from the Full Width at Half Wavelength

(FWHW) of x-ray peak lines of plane orientation using

the Debye-Scherrer formula;

$$D = \frac{0.94\lambda}{\beta cos\theta} \quad (1)$$

where; D = mean crystallite size

λ = wavelength of radiation (incident x-ray) used=0.15418

β = peak (line) broadening at half the maximum intensity

θ = Bragg angle (diffracted angle) in radians

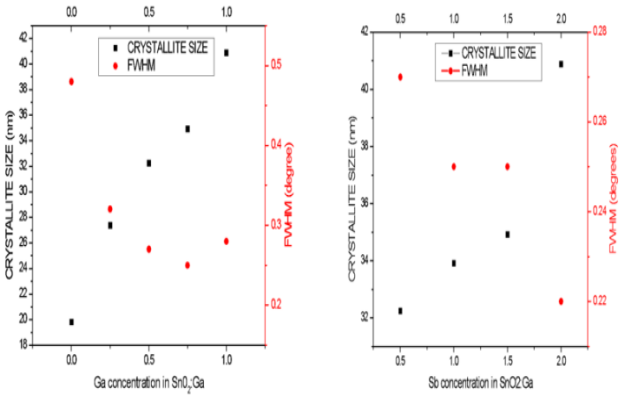

Figure 6. Crystallite size and FWHM Variation with dopant concentration

An observed improvement in average crystallite sizes is noted as the doping concentrations increase for both the Ga-doped and Sb-co-doped SnO_2 thin films. Specifically, the grain sizes of the thin films exhibit an increase from 19.83 nm to 32.24 nm for the Ga-doped tin oxide thin films and from 33.91 nm to 40.88 nm for the Sb-co-doped SnO_2 films with increasing concentrations of Ga and Sb. Additionally, the Full Width at Half Maximum (FWHM) of all the films decreases with an increase in precursor concentration, indicating enhanced crystallinity of the thin films.

This observed increase in crystallite sizes and decrease in FWHM is attributed to the reduced strain on the surface of the films. This reduction in strain occurs because the dopants act as nucleation sites in nanoparticle synthesis, thereby lowering the energy required for particles to initiate formation. Similar results of increased crystallite sizes with doping have been reported in studies by Rahul *et al*. [41] with doped ZnO and Ian E. *et al*. [42] regarding the effect of doping-induced aggregation on film morphology, as well as by Peddavarapu *et al*. [43] with SnO_2 thin films.

4. Conclusions

In conclusion, the observed increase in crystallite sizes upon doping of SnO_2 and Sb-co-Doped SnO_2;Ga thin films signifies enhanced crystallinity, which is essential for their optimal performance.. The presence of sharp and narrow diffractions in XRD spectra indicates a combination of crystalline and amorphous nature in the prepared thin films. Moreover, the increase in preferred orientations of the thin films corresponds to enhanced crystallite growth along specific planes. The intensification of film peaks with doping concentrations is attributed to the creation of sub-energy levels within the film lattice. Notably, a strong peak observed in all XRD spectra signifies a well-defined orientation of the thin films. The homogeneous grain sizes observed in SnO_2 and Sb-co-Doped SnO_2;Ga films contribute to their optimal electrical properties. Overall, doping concentrations significantly influence the structural properties of the prepared p-type TCO thin films of $SnO_2$and Sb-co-Doped SnO_2, confirming their suitability for high-quality device applications, particularly in solar cell technology which still records low efficiency.

References

[1] Marc R.M. (2021). Transparent Ceramics: Materials, Processing, Properties and Applications; *Encyclopedia of Materials; Technical Ceramics and Glasses*, 1:399-423.

[2] Hadjadj A., and Gilliot M. (2023).Recent Advances in Functional Transparent Semiconductor Films and coatings; Coating, 13:307.

[3] Pasquarelli R.M., Ginley D.S., and O'Hayre R. (2011). Solution Processing of transparent conductors from flask to film; *Chemical Society Reviews*, 40: 5406.

[4] Tyagi M., Tomar M., and Gupta V. (2013). P-N Junction of NiO Thin Film for Photonic Devices. *IEEE Electron Device Letters*, 34(1): 81-83.

[5] Jaehoon, P. (2018). Solution-Processed Gallium-Tin-Based oxide Semi-conductors for Thin Film Transistors; *Materials*, 11(1): 3390.

[6] Mageto J., Mwamburi M., and Muramba W. (2012). The influence of Al doping on optical, electrical and structural properties of transparent and conducting SnO_2:Al thin films prepared by spray pyrolysis technique. *Elixir Chemical Physics*, 53(2012): 11922-11927.

[7] Vikash K.R., Ganesh B.M., and Angshuman N. (2016). Band Edge Energies and Excitonic Transition Probabiities of Colloidal CsPbX3 Perovskite Nanocrystals; *ACS Energy Letter*, 1-20.

[8] Benjamin A.D., John B., Jennilee B., Simon A., Robert G., and David O. (2017). Engineering Valence Band Dispersion for High Mobility p-type Semiconductors; *Chemistry of Materials*, 29(6): 2402-2413.

[9] Hosono H. (2007). Recent progress in transparent oxide semiconductors: Materials and device application; *Thin Solid Films*, 515:6000-6014.

[10] Kelvin Z., Kai X., Mark G., and Russel E. (2016). P-type transparent conducting oxides. *Journal of Physics Condensed Matter*, 28(38): 383002.

[11] Liu X., Zhang N., Tang B., Li M., Zhang Y., Yu G., and Gong H. (2018). Highly Stable New Organic–Inorganic Hybrid 3D Perovskite CH3NH3PdI3 and 2D Perovskite (CH3NH3)3Pd2I7: DFT Analysis, Synthesis, Structure, Transition Behavior and Physical Properties. Journal of Physics and Chemistry Letters, 9(19): 5862–5872.

[12] Sathyamoorthy R., Abhirami M., Gokul B., Gautam S., Chae K., and Asokan K. (2014). Fabrication of p-n junction diode using SnO/SnO_2 thin films and its device characteristics. *Electron Materials Letters*, 10: 743-747.

[13] Hosono H., Hiramatsu H., Kamiya T., Tohei T., Ikenaga E., Mizoguchi T., Ikuhara Y., and Kobayashi K. (2010). Origins of hole doping and relevant optoelectronic properties of wide gap p-type semiconductor. *Journal of the American Chemical Society*, 132: 60-67.

[14] Fumiyasu O., and Yu K. (2018). Design and exploration of semiconductors from first principles: *A review of recent advances;* Applied Physics Express, 11:6.

[15] Kanghoon Y., Yong Y., Miso L., Dongsun Y., Joohee L., Sung H., and Seungwu H.(2018). Computational Discovery of p-type transparent oxide semiconductors using hydrogen descriptor; *Computational Materia*ls, 17: 4.

[16] Robertson J., and Falabretti B. (2011). Electronic Structure of Transparent Conducting Oxides. *In book*: *Handbook of Transparent Conductor. Springer*, 2: 27-50.

[17] Galatsisi K., Cukrov L., Wlodarski P., McCormick K., Kalantar-zadeh E., Cominic G.(2003). P- and n-type Fe-doped SnO_2 gas

sensors fabricated by the Mechano-chemical processing technique; *Sensors and Actuators B; Chemical*, 93: 532-565.

[18] Hsu C.L., Lu Y.C. (2012). Fabrication of a Transparent Ultraviolet Detector by using n-type Ga_2O_3 and p-type Ga-doped SnO_2 core-shell nanowires; *Journal of Nanoscale*, 4: 5710.

[19] Presley R.E., Munsee C.L., Park C.-H., Hong D., Wager J.F., and Keszler D.A. (2004). Tin Oxide Transparent Thin-Film Transistors; *Journal of Physics D: Applied Physics*, 37; 2810-2813.

[20] Chien-Yie Tsay, Chun-Wei Wu, Chien-Ming Lei, Fan-Shiong Chen and Chung-Kwei Lin (2010). Microstructural and Optical properties of Ga-doped ZnO Semiconductor Thin Films prepared by Sol-gel Process; *Thin Solid Films*. 519:1516-1520.

[21] Du J., and Ji Z.G. (2007). Effect of 1-Family Element Doping on Electronic Structures and Electrical Characteristics of SnO_2; *Acta Physica Sinica*, 56:2388-2392.

[22] Jain P., Singh S., Siddur A.M., and Srivastava A.K. (2012). Tin Oxide Thin Films Prepared by Thermal Evaporation Technique Under Different Vacuum Conditions; *Advanced Science, Engineering and Medicine*, 4: 230-236(7).

[23] Lee S.Y., and Park B.O. (2006). Structural, Electrical and Optical Characteristics of SnO2: Sb thin Films by Ultrasonic Spray Pyrolysis; Thin Solid Films, 510:154-158.

[24] Lu Y., Wang P., Zhang C.W., Feng X.Y., Jiang L., and Zhang G.L. (2011). First-principle on the Electronic and Optical properties of Mn-doped SnO2; Physica B: Condensed Matter, 406: 3137-3141.

[25] Kumar V., Govind A., and Ramarajan R. (2011). Optical and Photocatalytic Properties of Heavily F-Doped SnO_2 Nanocrystals by a Novel Single-Source Precursor Approach; *Journal of Inorganic Chemical society*, 50: 5637.

[26] Bagheri-Mohagheghi M.M., Shahtahamsebi N., Alinejad M.R., Youssef A., and Shokoon-Saremi M. (2009). Fe-doped SnO_2 transparent semi-conducting thin films deposited by spray pyrolysis technique: Thermoelectric and P-type conductivity properties; *Solid State Sciences*, 11: 233-239.

[27] Huang Y. Ji Z. and Chen C. (2007). Preparation and Characterization of p-type transparent conducting tin-gallium oxide films; *Applied Surface Science*, 253: 4819-4822.

[28] Kong J. (2007). Synthesis and properties of pure and antimony-doped tin dioxide thin films fabricated by sol-gel technique on silicon wafer. *Materials Chemistry and Physics*, 114(2): 854-859.

[29] Jia T., Wang W., Long F., Fu Z., Wang H., and Zhang Q. (2009). Synthesis, Characterization, and Photocatalytic Activity of Zn-Doped SnO_2 Hierarchical Architectures Assembled by Nanocones; *Journal of Physical Chemical society*, 113: 9071.

[30] Esro M., Georgakopoulos H., Lu H., Vourlias G., Krier A., Milne W.I., Gillian W.R., and Adamopoulos G.(2016). Solution Processed SnO_2:Sb Transparent Conductive Oxide as alternative to indium tin oxide for applications in organic light emitting diodes; *Journal of Material Chemical Society*, 4: 3563-3570.

[31] Jago T., Eva G.B., Rocio O., Oihane H., Lucia M., and Javier B. (2021). Indium Tin Oxide Thin Films Deposition by Magnetron Sputtering at Room Temperature for the Manufacturing of Efficient Transparent Heaters; *Coatings*, 11(1): 92.

[32] Jabbar H.K., Selma M.H., and Fadheela H.O. (2015). Preparation and Characterization of Tin Oxide Thin Films by Using spray pyrolysis Technique; *Engineering and Technology Journal*, 33(3B).

[33] Sapna D.P., Benjamin A.D., Sanjayan S., David O.S., Ivan P.P., and Claire J.C. (2018). Enhanced Electrical Properties of Antimony doped tin oxide thin films deposited via aerosol assisted chemical vapour deposition; *Journal of Materials Chemistry*.

[34] Jadhav H., Suryawanshi M.A., and Sinha S. (2017). Pulsed Laser Deposition of tin oxide thin films for emission studies; Applied Surface Science, 419: 764-769.

[35] Aravin P.P., Mohanapriya V. Dana K., Jiri M. (2020). Progress in Sol-gel Technology for the Coatings of fabrics; *Material-Academic Open Access Publishing*, 13(8): 1838.

[36] Anna L., Alessandon C. and Maurizio F. (2017). Active Sol-Gel Materials, Fluorescence spectra, and Lifetimes. In: Klein L., Aparicio M., Jitianu A. (eds) Handbook of Sol-Gel Science and Technology, 1: 1-43.

[37] Exarhos G. (2007). Discovery-based design of Transparent Conducting Oxide Films; *Materials Science Thin Solid Films*, 515(18): 7025-7052.

[38] Fredric S. (2018). Sol-Gel Technologies for Glass producers and users: Cleaning glass substrates. *Sprinker*, 3293: 19-34.

[39] Soraya H., Saeed R., and Suraya A. (2015). Grafting Carbon Nanotubes on Glass fiber by Dip-Coating Technique to enhance Tensile and Interfacial Shear Strength; *Journal of Nanomaterials*, 2015(7): 1497360.

[40] Sudipta M., Skidder A., Md S., Md R., Md B. (2023). Morphological Evaluation and boosted photocatalytic activity of N-doped ZnO nanoparticles prepared via co-precipitation method; *Science Direct*, 9: 10.

[41] Rahul S., Abhishek K., Bibhuti B. (2021). Influence of dopant concentration on powder morphology of photoluminescence characteristics of red-emitting Eu^{3+}- doped ZnO. Optik; 247: 5-6.

[42] Ian E., Erik W., Julia L., Tayane N.,John D., Jun Li., Gwangwu Z., Matthew P., Mark M., Adam J. (2016). Comparison of soln-mixed and sequencially processed P3HT.F4TCNO films: Effect of doping-induced aggregation on film morphology; Journal of materials Chemistry C., 10: 4-6.

[43] Peddavarapu S., Harish S.A., Ranjeth T., Srinvas G., Nagaiah K., Nanda N. (2021).Influence of Ga doping on Structural, Optical and Electrical properties of Transparent Conducting SnO_2 Thin Films; *Optik*, 226: 165859.